Lu *et al. Applied Biological Chemistry* (2022) 65:57
https://doi.org/10.1186/s13765-022-00726-6

KSABC
The Korean Society for Applied Biological Chemistry

ARTICLE Open Access

Circ_0026359 induces HOXA9 to regulate gastric cancer malignant progression through miR-140-3p

Shuirong Lu[1†], Jinlai Lu[1†], Lang Liu[2], Yilong Sun[2], Yixuan Zhao[2], Xi Tan[2] and Jingze Li[2*]

Abstract

Recent researches indicate the key role of circRNA in gastric cancer (GC) progression. However, the role of circ_0026359 in GC progression remains unclear. This study aims to analyze the role of circ_0026359 in GC development and the underlying mechanism. The results showed that compared with controls, GC tissues and cells displayed high circ_0026359 and HOXA9 expression, and low miR-140-3p expression. Depletion of circ_0026359 repressed cell proliferation, migration, invasion and glycolysis, and induced cell apoptosis. Circ_0026359 knockdown inhibited neoplasm growth in vivo. Under-expression of miR-140-3p, a target miRNA of circ_0026359, relieved the effects of circ_0026359 knockdown on GC progression. Additionally, HOXA9 was regulated by the circ_0026359/miR-140-3p axis. Thus, circ_0026359 absence inhibited GC progression by miR-140-3p/HOXA9 pathway, which provided an effective therapeutic target for GC.

Highlights

1. Circ_0026359 was upregulated in GC tissue specimens.
2. Circ_0026359 knockdown inhibited GC progression.
3. Circ_0026359 was associated with miR-140-3p/HOXAP axis.

Keywords: GC, circ_0026359, miR-140-3p, HOXA9

Introduction

According to the statistics reported in 2018, gastric cancer (GC) is the 3rd leading cause of cancer-related death for the combination of both sexes globally [1]. GC malignant progression is commonly induced by some factors like smoking, excessive salt accumulation and transgenation [2, 3]. Owing to the improvement of nutrition intake and newly developed therapeutic strategies, the survival of GC cases has steadily increased [4]. However, the survival time is less than 1 year for advanced GC patients [5]. As a result, investigating the mechanism underlying GC development is necessary to develop efficient therapeutic strategies.

CircRNA stably exists in tissues and cells and has no 5' or 3' polarities structure [6]. CircRNA is formed by back-splicing events and is featured by a covalently closed cyclic structure [7]. CircRNAs show a great possibility in acting as cancer biomarkers owing to their high stability, abundance as well as conservation in different types of cancer cells. Additionally, some strategies based on circRNA levels have been suggested for

†Shuirong Lu and Jinlai Lu contribute to this work equally as co-first authors

*Correspondence: pnms5pq@163.com

[2] Department of Endoscopy Center, Shanghai East Hospital, Tongji University School of Medicine, Shanghai, China
Full list of author information is available at the end of the article

the therapy of GC [8–10]. CircRNA was also involved in the cellular processes of cancers [11], which suggested the key roles of circRNA in GC development. Most of them are able to mediate GC-linked signaling cascades by acting as sponges for microRNAs (miRNAs) [12–14]. Circ_0026359, located in chr12:52,628,938–52,642,709 + and generated from keratin 7 (KRT7), is significantly upregulated in GC tissues than most other circRNAs, as compared with normal gastric tissues [15]. Given that circ_0026359 is associated with cisplatin sensitivity in GC [16], the circRNA is chosen for further study.

MiRNA virtually participates in post-transcriptional regulation and inhibits gene expression by targeting non-coding sequence of interest gene [17]. Abnormal miRNA level is associated as the main mechanism behind the pathophysiological processes of cancers, including GC [18]. Owing to its stability as well as easy and reproducible production, miRNA has the potential as a biomarker in GC [19, 20]. The above evidence manifest the importance of miRNA in GC development. Based on bioinformatics predictions, we found miR-140-3p might be a target miRNA of circ_0026359, and homeobox A9 (HOXA9) might be targeted by miR-140-3p. Importantly, previous data have shown that miR-140-3p acts as a repressor and HOXA9 knockdown inhibits cell proliferation and metastasis in GC [21, 22]. These data imply the possibility of circ_0026359/miR-140-3p/HOXA9 pathway regulating GC malignant progression; however, there is no study focusing on the role of the potential mechanism in gastric cancer progression.

Thus, whether circ_0026359 role in GC cell processes was attributed to miR-140-3p/HOXA9 axis was explored in the study. The molecular mechanism of the circRNA mediating GC development was tried to determine using the circ_0026359/miR-140-3p/HOXA9 signaling cascade.

Materials and methods

Clinical samples

With the approval of the Ethics Committee of the First People's Hospital of JingMen, we collected GC tissues (N = 30) and matched normal gastric tissues (N = 30) from GC patients during surgery in the First People's Hospital of JingMen. The signed written informed consent was provided by the GC sufferers. All tissues were kept at -80 °C.

Cell culture

Procell (Wuhan, China) provided human AGS cells, HGC-27 cells, and GES1 cells. AGS cells were maintained in Ham's F12K (Procell), and other types of cells were cultured in RPMI-1640 (Biosun, Shanghai, China) at 37 °C.

Vector establishment and cell transfection

GC cells at ~ 70% confluence were selected for cell transfection using TurboFect reagent (Thermo Fisher, Waltham, MA, USA) in accordance with the standard instructions. GenePharma (Shanghai, China) provided the small hairpin RNA targeting circ_0026359 (sh-circ_0026359, 5'-GATCCGTGATCCACGTGG TGCGGTTTCAAGAG AAACCGCACCACGTGGAT CACTTTTTG-3' and 5'-AATTCAAAAAGTGATCCA CGTGGTGCGGTTTCACTTC AAACCGCACCAC GTGGATCACG-3'), the mimics and inhibitors of miR-140-3p (miR-140-3p, 5'-UACCACAGGGUAGAACCA CGG-3' and anti-miR-140-3p, 5'-CCGUGGUUCUAC CCUGUGGUA-3'), and the respective controls. The coding sequence of HOXA9 generated by polymerase chain reaction (PCR) as well as pcDNA 3.0 vector (pcDNA; Genomeditech; Shanghai, China) were used to build HOXA9 overexpression plasmid (HOXA9).

qRT-PCR

The extracted RNA using TsingZol (Tsingke, Shanghai, China) was employed for reverse transcription with EasyScript® cDNA Synthesis SuperMix (TransGen, Beijing, China) or miRNA reverse transcription reagents (TaKaRa, Dalian, China). An aliquot of 50–80 ng cDNA was reacted on a Bio-Rad 96-well Machine with qRT-PCR Mix (Tsingke) to perform a quantification analysis of circRNA/miRNA/mRNA. Finally, gene expression was analyzed using the $2^{-\Delta\Delta Ct}$ method. The primer sequences are displayed in Table 1.

Identification of circ_0026359 location and stability

Circ_0026359 location was confirmed by the nucleocytoplasmic separation assay. In brief, the cultured GC cells were lysed on ice. Then, the PARIS™ Kit (Thermo Fisher)

Table 1 The sequences of forward (F) and reverse (R) primers used in this research

Gene	Sequences of primers (From 5' to 3')
circ_0026359-F	CACCACCCACAATCACAA
circ_0026359-R	TCTGCTGCTCCAGAAACC
KRT7-F	CATCGAGATCGCCACCTACC
KRT7-R	TGGAGAAGCTCAGGGCATTG
miR-140-3p-F	GCGCGTACCACAGGGTAGAA
miR-140-3p-R	AGTGCAGGGTCCGAGGTATT
HOXA9-F	TTGCACCAGACGAACAGTGA
HOXA9-R	AGCCCAATGGCGGTTTCATA
β-actin-F	CACCATTGGCAATGAGCGGTTC
β-actin-R	AGGTCTTTGCGGATGTCCACGT
U6-F	CTCGCTTCGGCAGCACA
U6-R	AACGCTTCACGAATTTGCGT

was used to extract nucleocytoplasmic RNA according to user's manual. Expression of nucleocytoplasmic circ_0026359 was confirmed by qRT-PCR.

For identifying the stability of circ_0026359, 50 ng/mL Actinomycin D (Seebio Biotech, Shanghai, China) was incubated with AGS and HGC-27 cells for different time points. Then, RNA was isolated, and circ_0026359 and KRT7 levels were detected by qRT-PCR.

Cell viability

GC cells were plated in tissue culture microplates, and treated with sh-circ_0026359, miR-140-3p, anti-miR-140-3p or HOXA9. Forty-eight hours later, cell counting kit-8 reagent (Abcam, Cambridge, MA, USA) was added into each well and incubated for 2 h. The absorbance at 460 nm (A460) was measured using a microplate reader (Thermo Fisher).

Cell colony formation assay

GC cells stably expressing plasmids or oligonucleotides were diluted in media and placed in 6-well plates. About 2-week culture later, cell supernatant was removed. Paraformaldehyde (Seebio Biotech) was used to incubate the cells. After the cells were washed twice with deionized water, the number of colonies containing > 50 cells was determined.

Flow cytometry analysis

The cells were fixed with ethanol (Millipore, Bradford, MA, USA) overnight at 4˚C, and then harvested. Afterward, staining buffer, propidium iodide (Beyotime, Shanghai, China) and RNase A (Beyotime) were incubated with the cells. Flow cytometer was employed to assess DNA content and cell apoptotic rate.

Western blot analysis

Protein Extraction Kit (Phygene, Fuzhou, China) was used to prepare protein lysates. After measuring protein concentration, protein samples were added into each lane of polyacrylamide gels. After that, skimmed milk (Solarbio, Beijing, China) was utilized to block aspecific signals, and the membranes were incubated with anti-CyclinD1 (1:100; Abcam), anti-Bax (1:800; Otwo Biotech, Shenzhen, China), anti-HOXA9 (1:800; Otwo Biotech), β-actin (1:1000; Abcam), and secondary antibodies (1:10,000; Abcam). The protein blots were developed using eyoECL Plus.

Transwell assay

Cells were suspended in FBS-free medium and dropwise added into the upper chambers coated with Matrigel (Corning, Madison, New York, USA). After 24 h later, the cells on the top surface of the lower chambers were treated with paraformaldehyde (Seebio Biotech) and crystal violet (Seebio Biotech), and photographed under a microscope (100 × ; Nikon, Tokyo, Japan). Cell migration assay was implemented in accordance with the above steps except that the upper chambers were not precoated with Matrigel.

Glucose consumption and lactate production

Cells were resuspended in Assay buffer (Abcam) and homogenized by pipetting up and down the tubes. Then, the supernatant was transferred to another tube, and endogenous LDH or enzymes were removed using Deproteinizing Sample Preparation Kit. The Reaction Mix or Background Reaction Mix was added into the test wells following the guidebook. Samples were assessed on microplate reader.

Mouse model assay

Under the agreement of the Animal Care and Use Committee of The First People's Hospital of JingMen, the assay was implemented on 12 five-week-old male BALB/c nude mice (Charles River, Beijing, China). These mice were randomized into 2 groups: (1) sh-con group (injected with AGS cells stably expressing sh-con); (2) sh-circ_0026359 group (injected with AGS cells with circ_0026359 knockdown). The above cell suspensions containing 5×10^6 cells were injected into the upper back of nude mice. The volume (V) of peritoneal nodules was monitored once a week. On the 28th day, mice were anesthetized with xylazine, the forming tumors were harvested. Stable AGS cell line was established by GenePharma Co., Ltd.

Immunohistochemistry (IHC) assay

Ki-67 expression was detected by IHC assay according to the published methods [23]. In short, the 4-μm-thick neoplasms from the mouse model assay were fixed, and dehydrated. The sections were heated at 80 °C and then incubated with anti-Ki-67 (1:80; Affinity, Nanjing, China) and secondary antibody (1:100; Affinity). Then, the samples were counterstained using hematoxylin (Phygene). The immunoreactivity was observed under a microscope.

Dual-luciferase reporter assay

The sequences of circ_0026359 and HOXA9 3'-untranslated region (3'UTR) containing the binding sites of miR-140-3p were amplified to establish the wild-type (WT) vectors (circ_0026359 WT and HOXA9 3'UTR WT). The mutant (MUT) plasmids including circ_0026359 MUT and HOXA9 3'UTR MUT were built by Yeasen (Shanghai, China). Then, the above vectors, miR-140-3p and miR-con were transfected into GC cells using TurboFect

reagent (Thermo Fisher). Fluorescence signals were detected using a Dual-Lucy Assay Kit (Solarbio).

Statistical analysis

The results from 3 independent duplicate assays were expressed as means ± standard deviations. The significant differences between the 2 groups with Student's *t*-tests or Wilcoxon rank-sum test, while among 3 or more groups with one-way analysis of variance. Log-rank test was used for comparing the disparities in overall survival curve, and a chi-square test was employed for comparing groups between low and high circ_0026359 expression. *P* value < 0.05 indicated statistical significance.

Results

Circ_0026359 expression in GC tissues and cells

As shown in Fig. 1A and B, circ_0026359 was overexpressed in GC tissues and AGS and HGC-27 cells when compared with the normal gastric tissues and human healthy gastric mucosa cells (GES1), respectively. Moreover, the patients with high circ_0026359 expression had a poorer overall survival (Fig. 1C). Meanwhile, circ_0026359 expression was significantly associated with tumor size, lymph node metastasis and tumor-node-metastasis stage in GC patients (Table 2). Subsequently, we found the high expression of circ_0026359 in the cytoplasm in comparison with its expression in cell nuclei (Fig. 1D and E), which suggested the circRNA mainly functioned in a post-transcriptional level. Further data exhibited that the transcript half-life of linear KRT7 was about 12 h, while that of circ_0026359 exceeded 36 h (Fig. 1F and G). Thus, circ_0026359 might be associated with GC progression.

Table 2 Correlation of clinicopathological features of GC patients with circ_0026359 expression levels

Characteristics	All cases	circ_0004585 expression		*p* value
		High	Low	
Age				0.449
≥ 60	19	8	11	
< 60	11	7	4	
Gender				0.143
Male	16	10	6	
Female	14	5	9	
Tumor size (cm)				0.027
< 4	17	5	12	
≥ 4	13	10	3	
Lymph node metestasis				0.009
Negative	18	5	11	
Positive	12	10	2	
TNM stage				0.007
I-II	20	6	14	
III-IV	10	9	1	

Chi-square test. *$P < 0.05$

Circ_0026359 knockdown inhibited AGS and HGC-27 cell tumor properties

Circ_0026359 expression was significantly downregulated by sh-circ_0026359 (Fig. 2A). Then, the study found

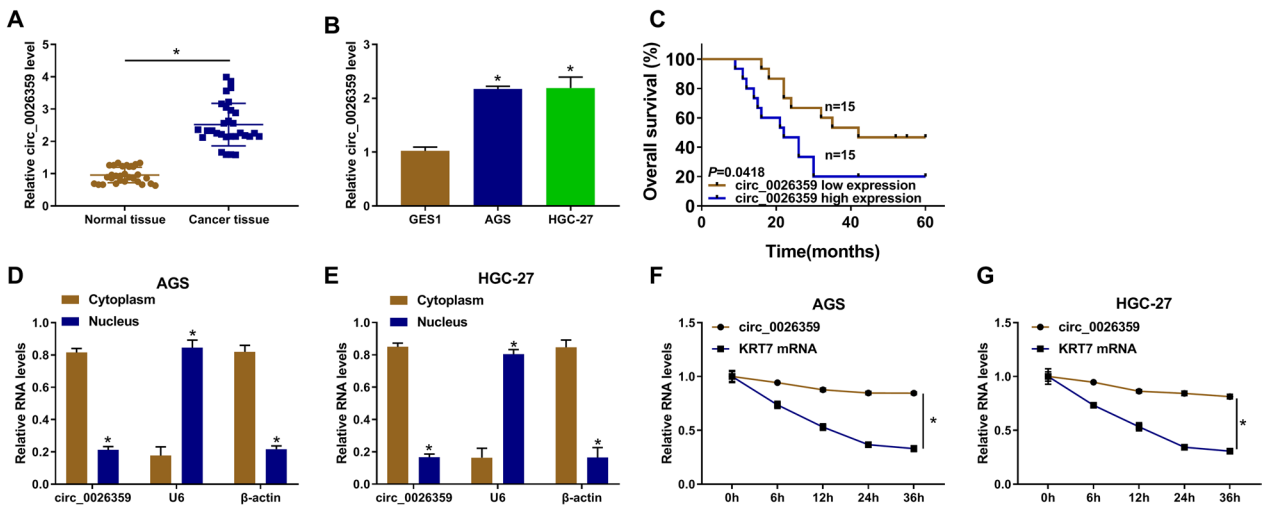

Fig. 1 The expression of circ_0026359 in GC tissues and cells. **A** and **B** The expression of circ_0026359 was detected by qRT-PCR in 30 pairs of GC and healthy gastric tissues as well as GES1, AGS and HGC-27 cells. **C** The association between circ_0026359 expression and the overall survival of GC patients. **D** and **E** Nucleocytoplasmic separation assay was performed to determine the location of circ_0026359 in AGS and HGC-27 cells. **F** and **G** The stability of circ_0026359 was confirmed by Actinomycin D treatment assay. *$P < 0.05$

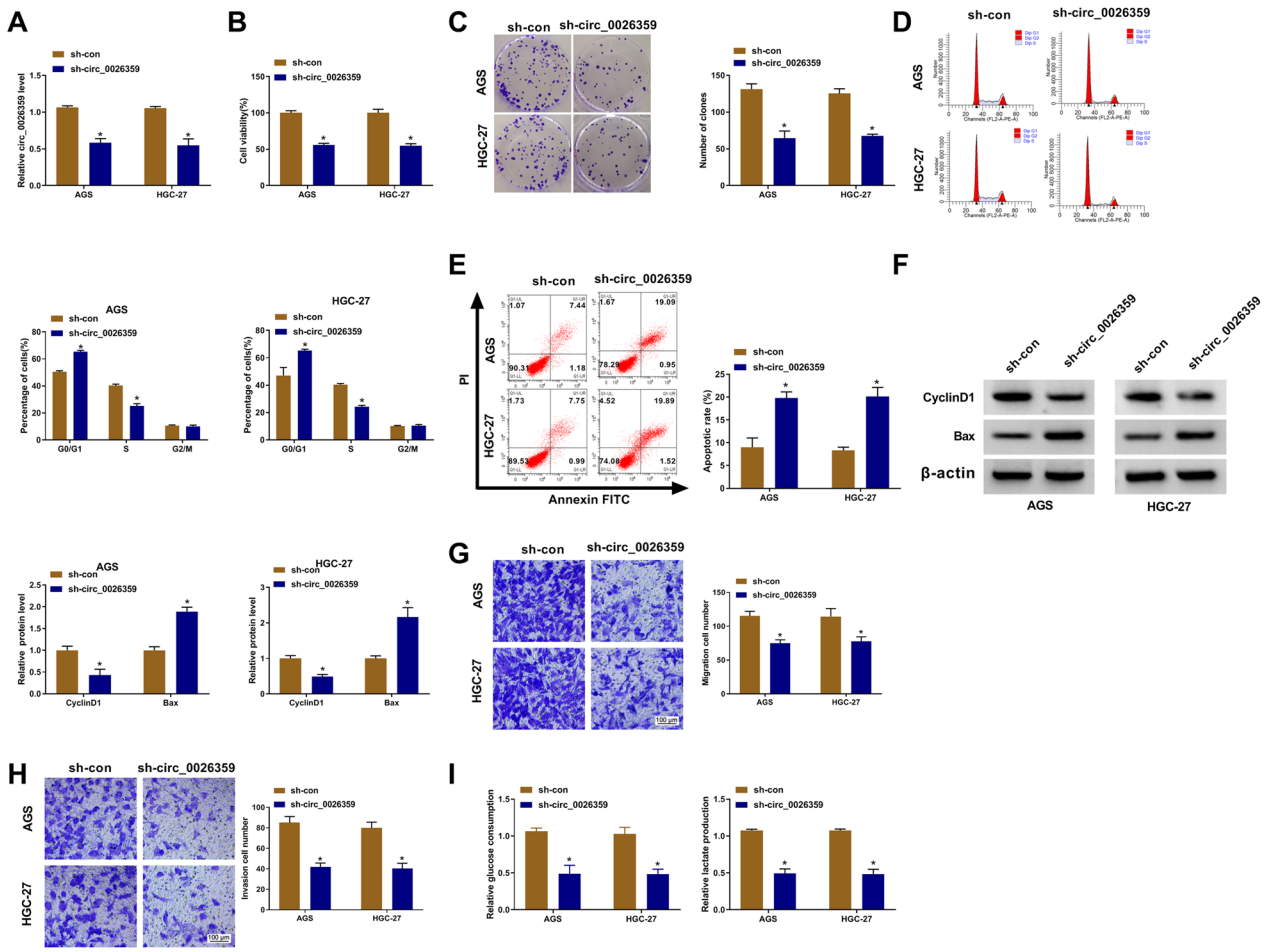

Fig. 2 The effects of circ_0026359 absence on GC cell growth. **A** The efficiency of circ_0026359 knockdown was detected by qRT-PCR in both AGS and HGC-27 cells. **B**–**I** AGS and HGC-27 cells were transfected with sh-circ_0026359 and sh-con, respectively. **B** CCK-8 assay was carried out to detect cell viability. **C** Colony formation assay was used to investigate cell colony-forming ability. **D** and **E** Cell cycle and apoptosis were analyzed by flow cytometry. **F** The protein expression of CyclinD1 and Bax was checked by western blot analysis. **G** and **H** Cell migration and invasion were evaluated by transwell assays. **I** Glucose and lactate assay kits were employed to detect glucose uptake and lactate production, respectively. $^{*}P < 0.05$

circ_0026359 depletion inhibited cell viability and cell proliferation (Fig. 2B-D). On the contrary, cell apoptosis was promoted by reducing circ_0026359 expression (Fig. 2E). In addition, circ_0026359 knockdown led to the downregulation of CyclinD1 and the upregulation of Bax (Fig. 2F), which certified the repressing role of circ_0026359 silencing in cell growth. Additionally, cell migration and invasion were inhibited by reducing circ_0026359 expression (Fig. 2G and H). Further, we found circ_0026359 absence inhibited glucose uptake and lactate production (Fig. 2I). Thus, all these findings demonstrated the repressing role of circ_0026359 knockdown in GC cell tumor properties.

Circ_0026359 silencing inhibited tumor formation in vivo

A mouse model assay was conducted to validate the repressing role of circ_0026359 silencing in GC cell processes. The volume and weight of the tumors from the sh-circ_0026359 group were smaller or lighter than in those tumors from the sh-con group (Fig. 3A and B). Comparative qRT-PCR analysis of the neoplasm samples displayed the reduced expression of circ_0026359 in the sh-circ_0026359 group (Fig. 3C). Additionally, it was found using IHC assay that the tumor samples from the sh-circ_0026359 group showed fewer Ki-67-positive cells (Fig. 3D). All in all, these observations elucidated circ_0026359 silencing inhibited tumor formation.

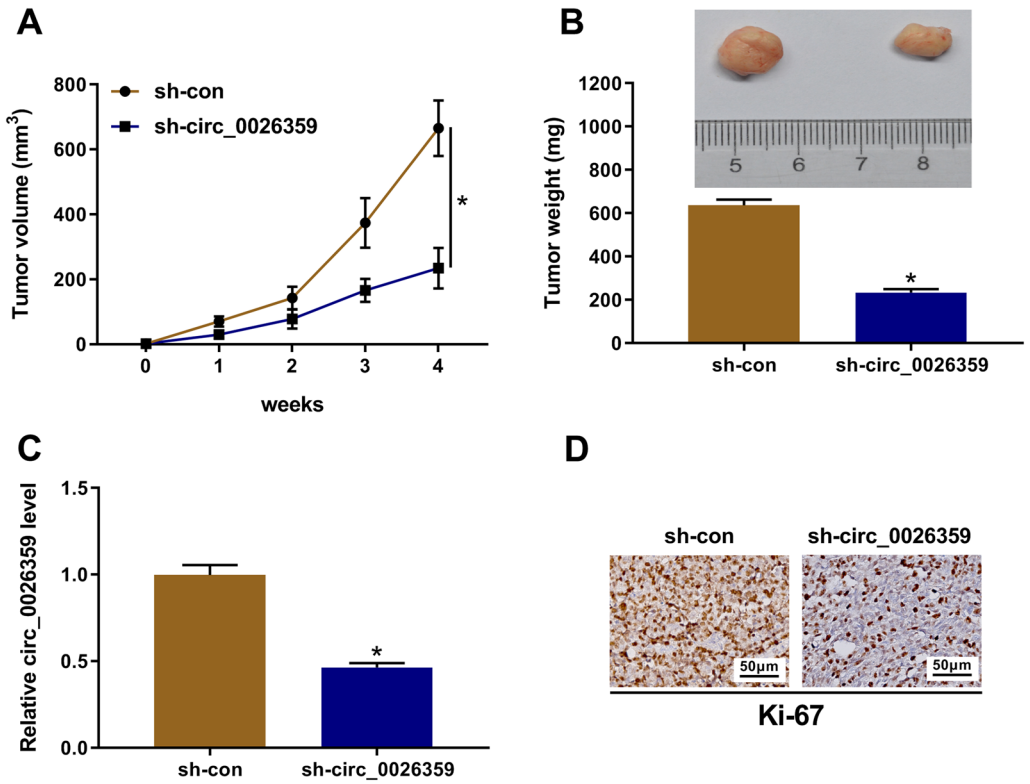

Fig. 3 The effect of circ_0026359 knockdown on tumor growth. **A** and **B** The effects of circ_0026359 silencing on the volume and weight of tumor samples. **C** Circ_0026359 expression was checked by qRT-PCR in tumor samples from sh-circ_0026359 and sh-con groups. **D** IHC assay was employed to determine the positive expression rate of Ki-67 in the forming tumors from sh-circ_0026359 and sh-con groups. **P* < 0.05

Circ_0026359 targeted miR-140-3p

The target miRNA of circ_0026359 was identified in this part. miR-140-3p could potentially bind to circ_0026359 (Fig. 4A). Subsequently, the luciferase activity of circ_0026359 WT was significantly inhibited by miR-140-3p mimics, but the luciferase activity of circ_0026359 MUT had no response to miR-140-3p overexpression (Fig. 4B and C). The above evidence demonstrated that circ_0026359 bound to miR-140-3p. Besides, the low expression of miR-140-3p was found in GC tissues and AGS and HGC-27 cells (Fig. 4D and E). Further, the study disclosed the negative correlation of circ_0026359 with miR-140-3p expression in clinical GC tissue specimens (Fig. 4F).

Circ_0026359 knockdown inhibited GC cell processes through miR-140-3p

We silenced circ_0026359 and miR-140-3p to demonstrate the consequential effect on GC cell processes. Comparative qRT-PCR analysis showed that miR-140-3p expression was significantly increased after circ_0026359 knockdown, where the effect was rescued after cotransfection of sh-circ_0026359 and miR-140-3p inhibitors (Fig. 5A). Then, we found the repressive effects of circ_0026359 silencing on cell viability and proliferation were attenuated after miR-140-3p absence (Fig. 5B-D). Consistently, miR-140-3p inhibitors restored circ_0026359 knockdown-induced cell apoptosis (Fig. 5 E). In support, the reduced expression of CyclinD1 and increased expression of Bax caused by circ_0026359 depletion were relieved by miR-140-3p inhibitors (Fig. 5F). Additionally, circ_0026359 absence-induced cell migration and invasion inhibition were remitted via decreasing miR-140-3p (Fig. 5G). Data from Fig. 5H exhibited that circ_0026359 knockdown decreased glucose consumption and lactate production, whereas miR-140-3p depletion counteracted these effects. Therefore, all data suggested circ_0026359 regulated GC cell processes by binding to miR-140-3p.

MiR-140-3p targeted HOXA9

HOXA9 carried the binding sites of miR-140-3p (Fig. 6A), and miR-140-3p mimics dramatically inhibited the luciferase activity of HOXA9 3'UTR WT rather than that of HOXA9 3'UTR MUT (Fig. 6B and C). Comparatively,

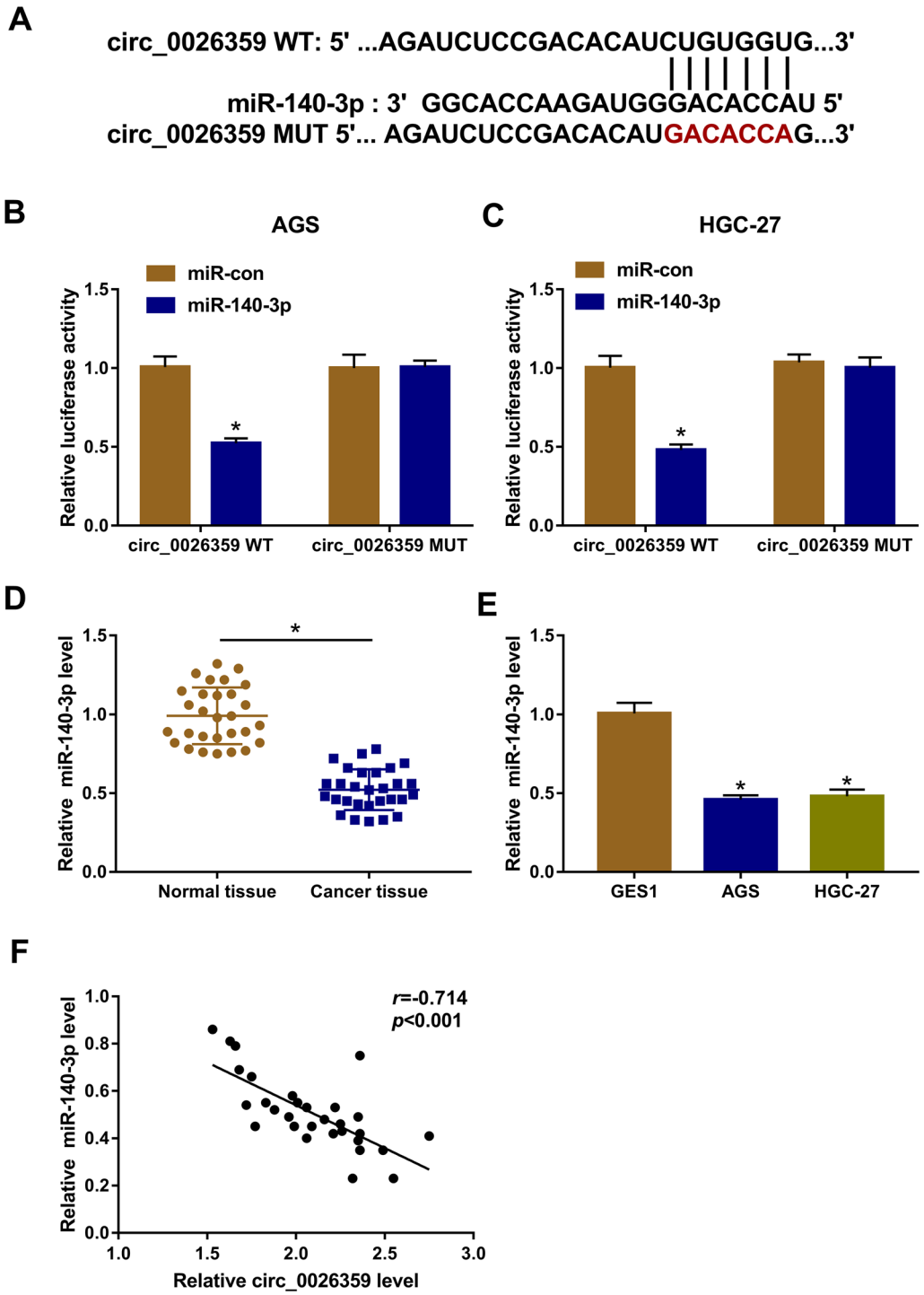

Fig. 4 Circ_0026359 was associated with miR-140-3p. **A** The schematic diagram showing the binding sites of circ_0026359 for miR-140-3p. **B** and **C** Dual-luciferase reporter assay was implemented to identify the targeting relationship between circ_0026359 and miR-140-3p. **D** and **E** MiR-140-3p expression was checked by qRT-PCR in GC tissues (N = 30), healthy gastric tissues (N = 30) and GES1, AGS and HGC-27 cells. **F** Spearman correlation analysis was employed to reveal the correlation between miR-140-3p and circ_0026359 expression in GC tissues. *$P < 0.05$

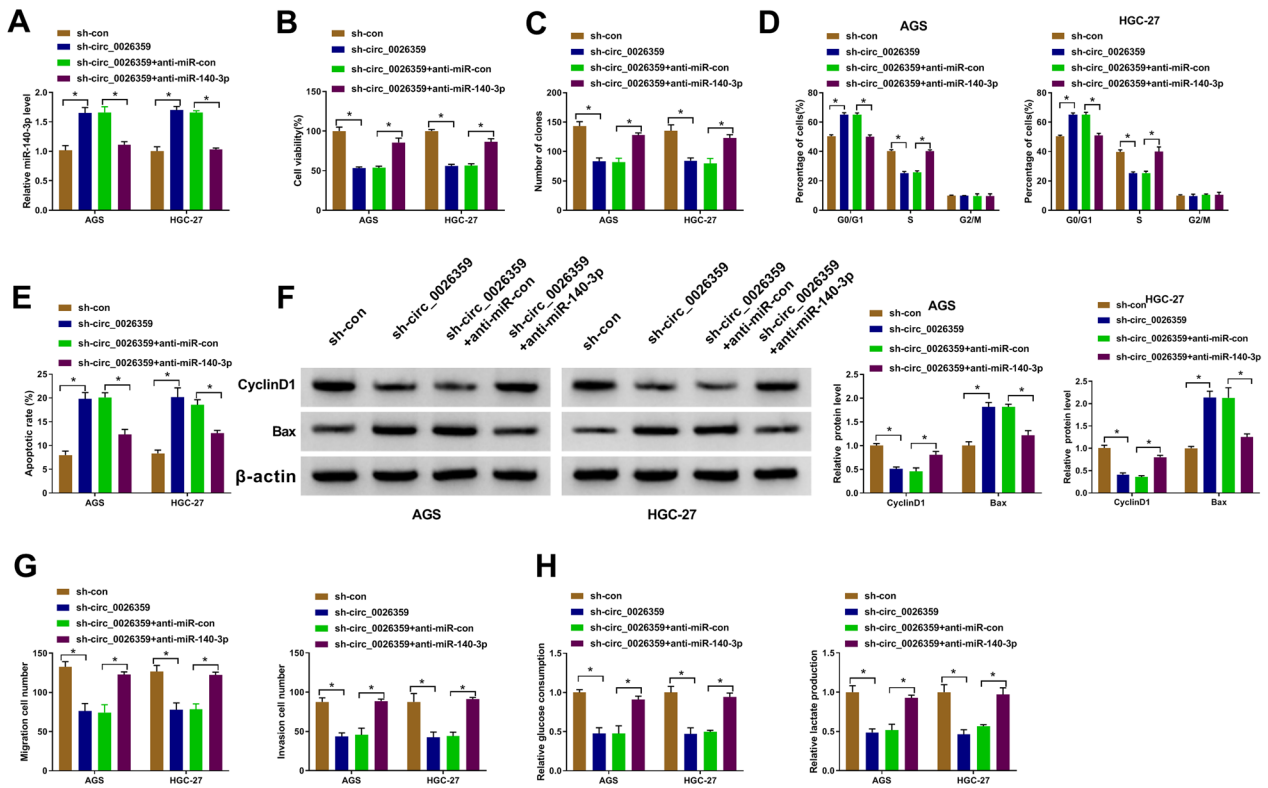

Fig. 5 The impacts between circ_0026359 knockdown and miR-140-3p inhibitors on GC cell processes. **A**–**H** Both AGS and HGC-27 cells were transfected with sh-con, sh-circ_0026359, sh-circ_0026359 + anti-miR-con and sh-circ_0026359 + anti-miR-140-3p, respectively. **A** MiR-140-3p expression was detected by qRT-PCR. **B** and **C** Cell viability and colony-forming ability were detected by CCK-8 and colony formation assays, respectively. **D** and **E** Cell cycle and apoptosis were demonstrated by flow cytometry analysis. **F** The protein levels of CyclinD1 and Bax were determined by western blot analysis. **G** Cell migration and invasion were evaluated by transwell assays. **H** Glucose and lactate assay kits were utilized to detect glucose uptake and lactate production, respectively. *$P < 0.05$

HOXA9 was highly expressed in GC tissues and cells (AGS and HGC-27) as compared with normal gastric tissues or GES1 cells (Fig. 6D, F and G). In support, we identified the negative correlation of miR-140-3p with HOXA9 expression in clinical GC tissues (Fig. 6E).

MiR-140-3p suppressed GC cell malignancy by negatively regulating HOXA9 expression

The high efficiency of miR-140-3p overexpression was shown in Fig. 7A. Then, miR-140-3p mimics reduced HOXA9 production, whereas the effect was relieved after upregulation of HOXA9 expression (Fig. 7B). Additionally, the decreased cell viability and proliferation by miR-140-3p were attenuated by increasing HOXA9 expression (Fig. 7C-E). The promoting effect of miR-140-3p mimics on cell apoptosis was also restored after HOXA9 introduction (Fig. 7F). In support, HOXA9 reintroduction relieved miR-140-3p-mediated CyclinD1 and Bax expression (Fig. 7G). Figure 7H showed that miR-140-3p mimics repressed cell migration and invasion, which was remitted by increasing HOXA9 expression. Moreover, HOXA9 overexpression rescued the inhibitory impacts of miR-140-3p mimics on glucose uptake and lactate production (Fig. 7I). By the large, all data manifested miR-140-3p regulated GC cell growth by binding to HOXA9.

Circ_0026359 regulated HOXA9 expression by interacting with miR-140-3p

To demonstrate whether circ_0026359 could regulate HOXA9 expression through miR-140-3p, we silenced circ_0026359 and miR-140-3p. Circ_0026359 absence reduced HOXA9 expression, but the effect was rescued by miR-140-3p inhibitors (Fig. 8A and B). The finding indicated that circ_0026359 regulated HOXA9 by associating with miR-140-3p.

Discussion

As compared to some other cancers, clinical outcome of GC sufferers remains unsatisfactory. Much work suggested the potential of circRNAs as therapeutic targets for GC. Cross-sectional researches indicate that a potential mechanistic route for circRNA to mediate malignant

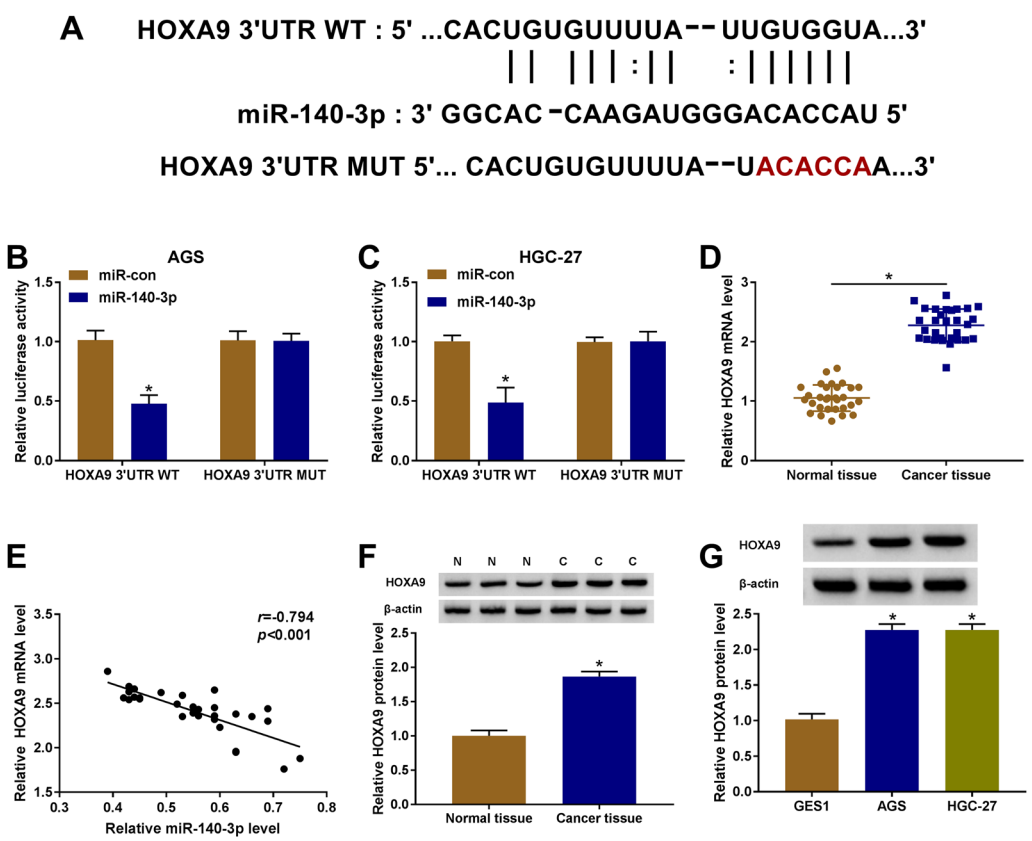

Fig. 6 MiR-140-3p bound to HOXA9. **A** The binding sites of miR-140-3p for HOXA9. **B** and **C** The connection of miR-140-3p and HOXA9 was identified by dual-luciferase reporter assay. **D** HOXA9 expression was detected by qRT-PCR in GC tissues and normal gastric tissues. **E** The linear correlation of miR-140-3p and HOXA9 was demonstrated by Spearman correlation analysis. **F** and **G** HOXA9 expression was detected by western blot in GC tissues, normal gastric tissues, GES1 cells, AGS cells and HGC-27 cells.*$P < 0.05$

progression of GC cells is to modulate mRNA and some signaling pathways via trapping miRNA [13, 24]. In this study, we found high circ_0026359 expression in GC patients and cells, and circ_0026359 silencing inhibited GC malignant progression. The underlying mechanism involved miR-140-3p and HOXA9.

The detailed mechanism related to circRNA in GC development has been partly unveiled. Circ_001569 contributed to GC cell proliferation by binding to miR-145 [25]. Circ_100782 accelerated GC cell motility by adsorbing miR-574-3p [26]. From the data of Fang and his colleagues, we found miR-149/Wnt1 feedback loop participated in circ_0044516-mediated GC cell growth [27]. Role of circ_0026359 in GC progression is rarely reported. Recent research displayed that poor survival of GC cases involved the increased expression of circ_0026359 [16]; however, the inner mechanism was unknown. In this research, we found that circ_0026359 was overexpressed in GC cases and cells, which was in line with the reported data [16]. Additionally, circ_0026359 expression was negatively associated with the overall survival of GC patients. Circ_0026359 silencing inhibited cell proliferation, metastasis and tumor formation, and promoted cell apoptosis. During cancer development, cancer cells are inclined to produce energy from glucose metabolism to resist metabolic stresses. The phenomenon is known as the "Warburg effect", which usually causes the increase of glucose uptake as well as accumulation of ATP and lactate production [28]. Herein, it was found that circ_0026359 absence repressed glycolysis in GC cells.

miR-140-3p carried the complementary sequence of circ_0026359, as determined by a bioinformatics tool. MiR-140-3p can repress the cell processes of colorectal cancer [29], cutaneous melanoma [30] and breast cancer [31]. In GC, Zhang and his colleagues indicated the low expression of miR-140-3p in GC tissues and proved that miR-140-3p inhibited GC cell growth through interaction with circRNA ATPase family AAA domain containing 1 (circATAD1) [32]. In addition, recent research unveiled that miR-140-3p impeded GC cell growth and metastasis by reducing B-cell lymphoma-2

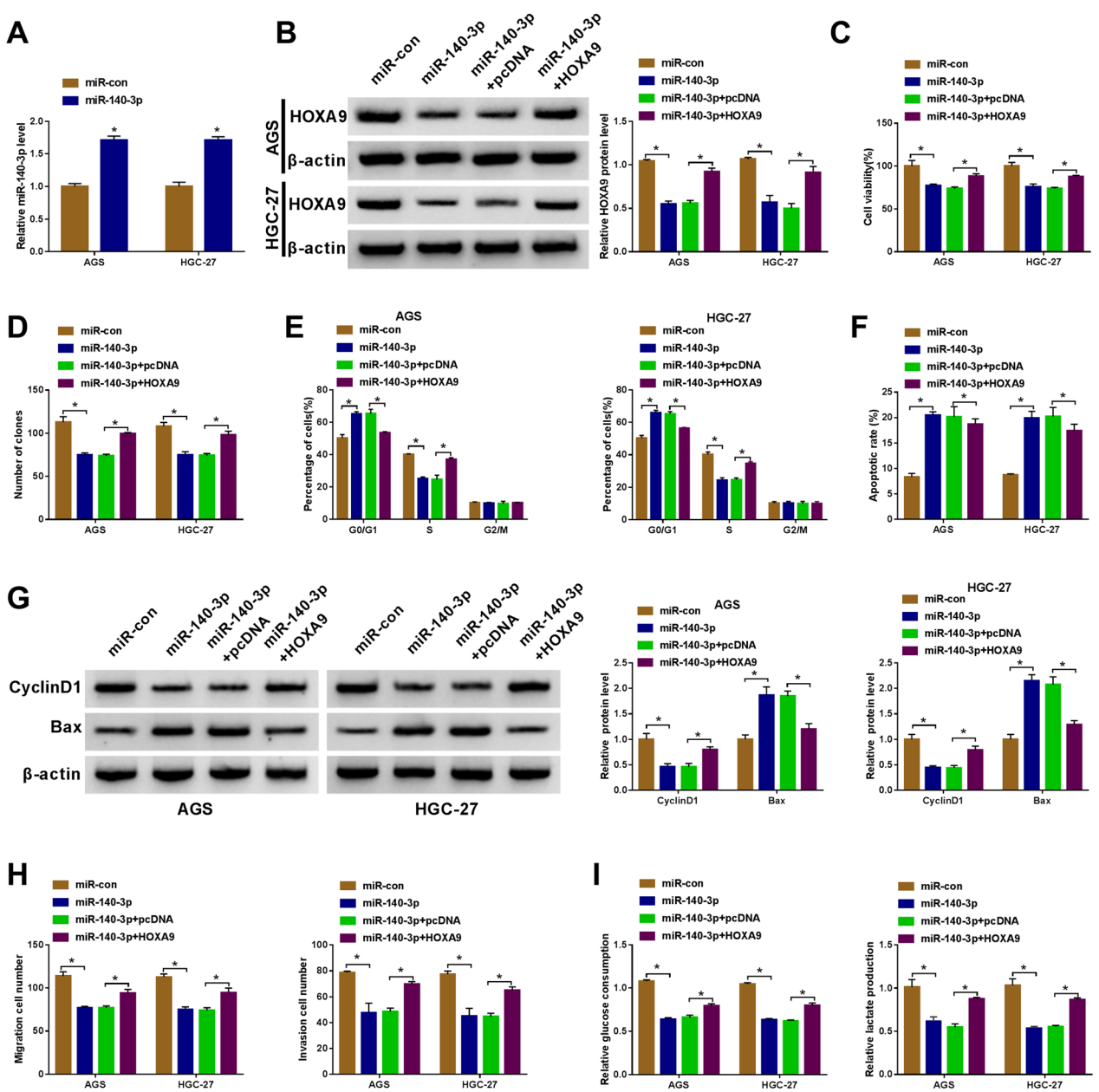

Fig. 7 HOXA9 overexpression attenuated the effects of miR-140-3p on GC cell processes. **A** The efficiency of miR-140-3p mimics in increasing miR-140-3p expression was determined by qRT-PCR. **B**–**I** AGS and HGC-27 cells were transfected with miR-con, miR-140-3p, miR-140-3p + pcDNA or miR-140-3p + HOXA9. **B** HOXA9 expression was detected by western blot analysis. **C** and **D** Cell viability and colony-forming ability were detected by CCK-8 assay and colony formation assay, respectively. **E** and **F** Cell cycle and apoptosis were demonstrated by flow cytometry analysis. **G** The protein levels of CyclinD1 and Bax were determined by western blot analysis. **H** Cell migration and invasion were evaluated by transwell assays. **I** Glucose and lactate assay kits were utilized to detect glucose uptake and lactate production, respectively. *$P < 0.05$

and increasing beclin 1 production [21]. Agreeing with the above data, the research also reported the repressing role of miR-140-3p in GC progression. Different from the published data, we found that miR-140-3p inhibited glycolysis. Importantly, the study provided evidence that circ_0026359 regulated GC development by absorbing miR-140-3p.

HOXA9 is a member of HOX genes and can encode proteins that play essential parts in regulating the development of cancers at an organismal and evolutionary

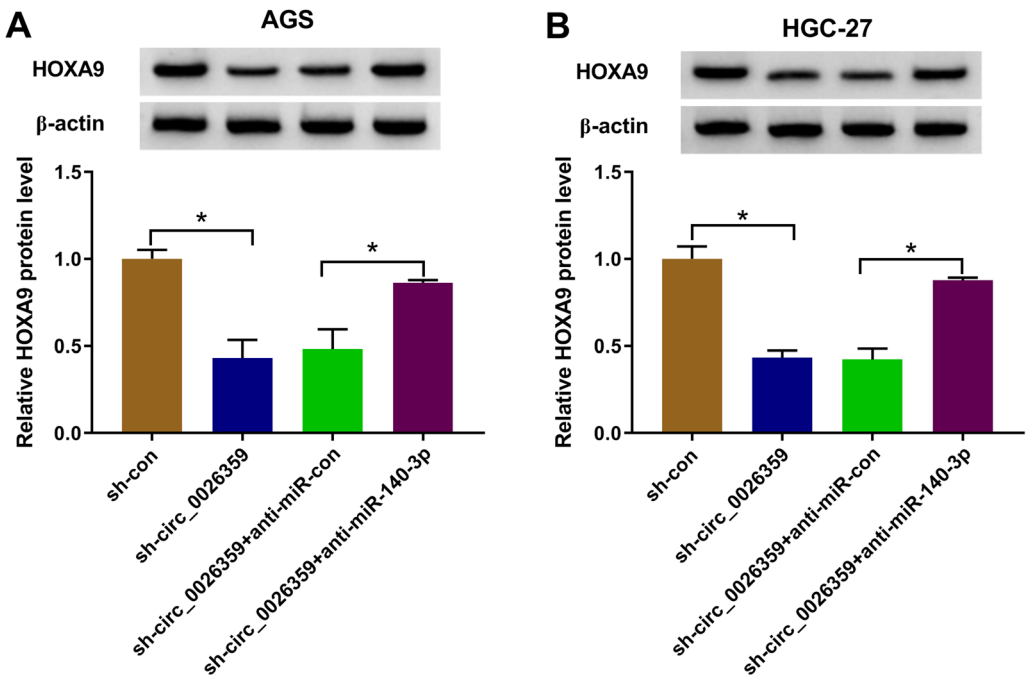

Fig. 8 The effects of circ_0026359 knockdown and miR-140-3p inhibitors on HOXA9 expression. **A** and **B** Western blot was performed to detect the impacts between circ_0026359 silencing and miR-140-3p inhibitors on the protein expression of HOXA9 in both AGS and HGC-27 cells. *$P < 0.05$

level. Based on our reviews of literature, HOXA9 is one of the most commonly altered genes in cancer progression [33]. Previous reports demonstrated that HOXA9 acted as a suppressor in the progression of cutaneous squamous cell carcinoma [34], and breast cancer [35], and had an oncogenic function in hematologic cancer [36] and osteosarcoma [37]. According to the data reported in 2017, HOXA9 was upregulated in GC tissues and was related to lymphaden metastasis, cell differentiation, and poor clinical outcome of GC patients [38]. The data from Yu et al. implied that HOXA9 increased GC cell proliferation and metastasis [22]. Agreeing with the above opinions, our data also reported the augment of HOXA9 expression in gastric cancer tissue specimens and the promoting effects of HOXA9 on cellular proliferation and motility. Beyond that, the study also showed that HOXA9 inhibited cell apoptosis and promoted glucose metabolism. Very importantly, the study elucidated that HOXA9 promoted GC cell growth via binding to miR-140-3p. Also, circ_0026359 mediated HOXA9 expression through the regulation of miR-140-3p.

However, the data about the function of miR-140-3p/HOAX9 in tumor tumorigenesis of GC in vivo are lacking in the present research. Additionally, the relevant clinical trials verifying the novel mechanism are absent in this research.

Abbreviations

GC: Gastric cancer; miRNA: MicroRNA; KRT7: Keratin 7; HOXA9: Homeobox A9; PCR: Polymerase chain reaction; IHC: Immunohistochemistry; 3′UTR : 3′-Untranslated region; circATAD1: CircRNA ATPase family AAA domain containing 1.

Supplementary Information

The online version contains supplementary material available at https://doi.org/10.1186/s13765-022-00726-6.

Additional file 1: Figure S1. The underlying mechanism of circ_0026359 regulating GC progression. The pathogenesis of GC involved high circ_0026359 upregulated. The increased circ_0026359 expression induced HOXA9 production in a miR-140-3p-dependent manner, further increasing GC cell proliferation, migration, invasion and glycolysis and decreasing cell apoptosis.

Acknowledgements

Not applicable.

Author contributions

Conceptualization and Methodology: JL and LL; Formal analysis and Data curation: YS, YZ and XT; Validation and Investigation: SL and JL; Writing—original draft preparation and Writing—review and editing: SL, JL, LL and YiS; All authors read and approved the final manuscript.

Funding

This work was supported by Top-Level Clinical Discipline Project of Shanghai Pudong (PWYgf 2018–04).

Availability of data and materials
The analyzed data sets generated during the present study are available from the corresponding author on reasonable request.

Declarations

Ethics approval and consent to participate
The present study was approved by the ethical review committee of Shanghai East Hospital, Tongji University School of Medicine. Written informed consent was obtained from all enrolled patients.

Consent for publication
Patients agree to participate in this work

Competing interests
The authors declare that they have no competing interests.

Author details
[1]Department of Gastroenterology, Shanghai East Hospital, Tongji University School of Medicine, 1800 Yuntai Road, Pudong New Area, Shanghai 200120, China. [2]Department of Endoscopy Center, Shanghai East Hospital, Tongji University School of Medicine, Shanghai, China.

Received: 18 May 2022 Accepted: 4 August 2022
Published online: 22 August 2022

References

1. Bray F, Ferlay J, Soerjomataram I, Siegel RL, Torre LA, Jemal A (2018) Global cancer statistics 2018: GLOBOCAN estimates of incidence and mortality worldwide for 36 cancers in 185 countries. CA Cancer J Clin 68(6):394–424. https://doi.org/10.3322/caac.21492
2. Funakoshi T, Miyamoto S, Kakiuchi N, Nikaido M, Setoyama T, Yokoyama A, Horimatsu T, Yamada A, Torishima M, Kosugi S et al (2019) Genetic analysis of a case of Helicobacter pylori-uninfected intramucosal gastric cancer in a family with hereditary diffuse gastric cancer. Gastric Cancer 22(4):892–898. https://doi.org/10.1007/s10120-018-00912-w
3. Ge S, Feng X, Shen L, Wei Z, Zhu Q, Sun J (2012) Association between habitual dietary salt intake and risk of gastric cancer: a systematic review of observational studies. Gastroenterol Res Pract 2012:808120. https://doi.org/10.1155/2012/808120
4. Sitarz R, Skierucha M, Mielko J, Offerhaus GJA, Maciejewski R, Polkowski WP (2018) Gastric cancer: epidemiology, prevention, classification, and treatment. Cancer Manag Res 10:239–248. https://doi.org/10.2147/cmar.S149619
5. Bang YJ, Van Cutsem E, Feyereislova A, Chung HC, Shen L, Sawaki A, Lordick F, Ohtsu A, Omuro Y, Satoh T et al (2010) Trastuzumab in combination with chemotherapy versus chemotherapy alone for treatment of HER2-positive advanced gastric or gastro-oesophageal junction cancer (ToGA): a phase 3, open-label, randomised controlled trial. Lancet 376(9742):687–697. https://doi.org/10.1016/s0140-6736(10)61121-x
6. Li R, Wu B, Xia J, Ye L, Yang X (2019) Circular RNA hsa_circRNA_102958 promotes tumorigenesis of colorectal cancer via miR-585/CDC25B axis. Cancer Manag Res 11:6887–6893. https://doi.org/10.2147/cmar.S212180
7. Qu S, Yang X, Li X, Wang J, Gao Y, Shang R, Sun W, Dou K, Li H (2015) Circular RNA: a new star of noncoding RNAs. Cancer Lett 365(2):141–148. https://doi.org/10.1016/j.canlet.2015.06.003
8. Piwecka M, Glažar P, Hernandez-Miranda LR, Memczak S, Wolf SA, Rybak-Wolf A, Filipchyk A, Klironomos F, Cerda Jara CA, Fenske P et al (2017) Loss of a mammalian circular RNA locus causes miRNA deregulation and affects brain function. Science. https://doi.org/10.1126/science.aam8526
9. Yao Z, Luo J, Hu K, Lin J, Huang H, Wang Q, Zhang P, Xiong Z, He C, Huang Z et al (2017) ZKSCAN1 gene and its related circular RNA (circZKSCAN1) both inhibit hepatocellular carcinoma cell growth, migration, and invasion but through different signaling pathways. Mol Oncol 11(4):422–437. https://doi.org/10.1002/1878-0261.12045
10. Yu L, Gong X, Sun L, Zhou Q, Lu B, Zhu L (2016) The Circular RNA cdr1as act as an oncogene in hepatocellular carcinoma through targeting miR-7 expression. PLoS ONE 11(7):e0158347. https://doi.org/10.1371/journal.pone.0158347
11. Li R, Jiang J, Shi H, Qian H, Zhang X, Xu W (2020) CircRNA: a rising star in gastric cancer. Cell Mol Life Sci 77(9):1661–1680. https://doi.org/10.1007/s00018-019-03345-5
12. Xie M, Yu T, Jing X, Ma L, Fan Y, Yang F, Ma P, Jiang H, Wu X, Shu Y et al (2020) Exosomal circSHKBP1 promotes gastric cancer progression via regulating the miR-582-3p/HUR/VEGF axis and suppressing HSP90 degradation. Mol Cancer 19(1):112. https://doi.org/10.1186/s12943-020-01208-3
13. Zhang X, Wang S, Wang H, Cao J, Huang X, Chen Z, Xu P, Sun G, Xu J, Lv J et al (2019) Circular RNA circNRIP1 acts as a microRNA-149-5p sponge to promote gastric cancer progression via the AKT1/mTOR pathway. Mol Cancer 18(1):20. https://doi.org/10.1186/s12943-018-0935-5
14. Zhang Y, Liu H, Li W, Yu J, Li J, Shen Z, Ye G, Qi X, Li G (2017) CircRNA_100269 is downregulated in gastric cancer and suppresses tumor cell growth by targeting miR-630. Aging (Albany NY) 9(6):1585–1594. https://doi.org/10.18632/aging.101254
15. Zhang Y, Han T, Li J, Cai H, Xu J, Chen L, Zhan X (2020) Comprehensive analysis of the regulatory network of differentially expressed mRNAs, lncRNAs and circRNAs in gastric cancer. Biomed Pharmacother 122:109686. https://doi.org/10.1016/j.biopha.2019.109686
16. Zhang Z, Yu X, Zhou B, Zhang J, Chang J (2020) Circular RNA circ_0026359 enhances cisplatin resistance in gastric cancer via targeting miR-1200/POLD4 pathway. Biomed Res Int 2020:5103272. https://doi.org/10.1155/2020/5103272
17. Krol J, Loedige I, Filipowicz W (2010) The widespread regulation of microRNA biogenesis, function and decay. Nat Rev Genet 11(9):597–610. https://doi.org/10.1038/nrg2843
18. Ali Syeda Z, Langden SSS, Munkhzul C, Lee M, Song SJ (2020) Regulatory mechanism of MicroRNA expression in cancer. Int J Mol Sci 21(5):1723. https://doi.org/10.3390/ijms21051723
19. Link A, Kupcinskas J (2018) MicroRNAs as non-invasive diagnostic biomarkers for gastric cancer: current insights and future perspectives. World J Gastroenterol 24(30):3313–3329. https://doi.org/10.3748/wjg.v24.i30.3313
20. Link A, Kupcinskas J, Wex T, Malfertheiner P (2012) Macro-role of microRNA in gastric cancer. Dig Dis 30(3):255–267. https://doi.org/10.1159/000336919
21. Chen J, Cai S, Gu T, Song F, Xue Y, Sun D (2021) MiR-140–3p impedes gastric cancer progression and metastasis by regulating BCL2/BECN1-Mediated autophagy. Onco Targets Ther 14:2879–2892. https://doi.org/10.2147/ott.S299234
22. Yu J, Tian X, Chang J, Liu P, Zhang R (2017) RUNX3 inhibits the proliferation and metastasis of gastric cancer through regulating miR-182/HOXA9. Biomed Pharmacother 96:782–791. https://doi.org/10.1016/j.biopha.2017.08.144
23. Li T, Zhou W, Li Y, Gan Y, Peng Y, Xiao Q, Ouyang C, Wu A, Zhang S, Liu J et al (2019) MiR-4524b-5p/WTX/β-catenin axis functions as a regulator of metastasis in cervical cancer. PLoS ONE 14(4):e0214822–e0214822. https://doi.org/10.1371/journal.pone.0214822
24. Luo Z, Rong Z, Zhang J, Zhu Z, Yu Z, Li T, Fu Z, Qiu Z, Huang C (2020) Circular RNA circCCDC9 acts as a miR-6792-3p sponge to suppress the progression of gastric cancer through regulating CAV1 expression. Mol Cancer 19(1):86. https://doi.org/10.1186/s12943-020-01203-8
25. Shen F, Liu P, Xu Z, Li N, Yi Z, Tie X, Zhang Y, Gao L (2019) CircRNA_001569 promotes cell proliferation through absorbing miR-145 in gastric cancer. J Biochem 165(1):27–36. https://doi.org/10.1093/jb/mvy079
26. Xin D, Xin Z (2020) CircRNA_100782 promotes roliferation and metastasis of gastric cancer by downregulating tumor suppressor gene Rb by adsorbing miR-574–3p in a sponge form. Eur Rev Med Pharmacol Sci. 24(17):8845–8854
27. Fang J, Chen W, Meng X (2020) Downregulating circRNA_0044516 inhibits cell proliferation in gastric cancer through miR-149/Wnt1/β-catenin pathway. J Gastrointest Surg. https://doi.org/10.1007/s11605-020-04834-w
28. Fan C, Tang Y, Wang J, Xiong F, Guo C, Wang Y, Zhang S, Gong Z, Wei F, Yang L et al (2017) Role of long non-coding RNAs in glucose metabolism in cancer. Mol Cancer 16(1):130–130. https://doi.org/10.1186/s12943-017-0699-3

29. Jiang W, Li T, Wang J, Jiao R, Shi X, Huang X, Ji G (2019) miR-140–3p suppresses cell growth and induces apoptosis in colorectal cancer by targeting PD-L1. Onco Targets Ther 12:10275–10285. https://doi.org/10.2147/ott.S226465
30. He Y, Yang Y, Liao Y, Xu J, Liu L, Li C, Xiong X (2020) miR-140–3p inhibits cutaneous melanoma progression by disrupting AKT/p70S6K and JNK pathways through ABHD2. Mol Ther Oncolytics 17:83–93. https://doi.org/10.1016/j.omto.2020.03.009
31. Zhou Y, Wang B, Wang Y, Chen G, Lian Q, Wang H (2019) miR-140-3p inhibits breast cancer proliferation and migration by directly regulating the expression of tripartite motif 28. Oncol Lett 17(4):3835–3841. https://doi.org/10.3892/ol.2019.10038
32. Zhang L, Chang X, Zhai T, Yu J, Wang W, Du A, Liu N (2020) A novel circular RNA, circ-ATAD1, contributes to gastric cancer cell progression by targeting miR-140-3p/YY1/PCIF1 signaling axis. Biochem Biophys Res Commun 525(4):841–849. https://doi.org/10.1016/j.bbrc.2020.02.100
33. Bhatlekar S, Fields JZ, Boman BM (2014) HOX genes and their role in the development of human cancers. J Mol Med (Berl) 92(8):811–823. https://doi.org/10.1007/s00109-014-1181-y
34. Han S, Li X, Liang X, Zhou L (2019) HOXA9 transcriptionally promotes apoptosis and represses autophagy by targeting NF-κB in cutaneous squamous cell carcinoma. Cells. https://doi.org/10.3390/cells8111360
35. Gilbert PM, Mouw JK, Unger MA, Lakins JN, Gbegnon MK, Clemmer VB, Benezra M, Licht JD, Boudreau NJ, Tsai KK et al (2010) HOXA9 regulates BRCA1 expression to modulate human breast tumor phenotype. J Clin Invest 120(5):1535–1550. https://doi.org/10.1172/jci39534
36. de Bock CE, Demeyer S, Degryse S, Verbeke D, Sweron B, Gielen O, Vandepoel R, Vicente C, Vanden Bempt M, Dagklis A et al (2018) HOXA9 cooperates with activated JAK/STAT signaling to drive leukemia development. Cancer Discov 8(5):616–631. https://doi.org/10.1158/2159-8290.Cd-17-0583
37. Zhang ZF, Li GR, Cao CN, Xu Q, Wang GD, Jiang XF (2018) MicroRNA-1294 targets HOXA9 and has a tumor suppressive role in osteosarcoma. Eur Rev Med Pharmacol Sci 22(24):8582–8588
38. Ma YY, Zhang Y, Mou XZ, Liu ZC, Ru GQ, Li E (2017) High level of homeobox A9 and PBX homeobox 3 expression in gastric cancer correlates with poor prognosis. Oncol Lett 14(5):5883–5889. https://doi.org/10.3892/ol.2017.6937

Publisher's Note